Available online www.jocpr.com

Journal of Chemical and Pharmaceutical Research, 2016, 8(7):373-384

Research Article

ISSN : 0975-7384
CODEN(USA) : JCPRC5

Optimization of fluidized bed carbochlorination of zirconia in pilot scale reactor

Mohammad Reza Ghasemi, Seyyed Mohammad Ghoreishi* and Mohammadhadi Jazini

Department of Chemical Engineering, Isfahan University of Technology, Isfahan 84156-83111, Iran

---

ABSTRACT

One of the most important units in the production of zirconiumis the chlorination reaction of zirconia in the presence of carbon in a fluidized bed reactor. An improved version of a pilot fluidized bed reactor with the production capacity of 10 kg per day was designed and built. In order to optimize the operating conditions of the reactor, the fluidized bed zirconia carbochlorination reactor was modeled via a two-phase hydrodynamic model. The model was developed according to the hypothesis of plug (P) for the bubble and mixed (M) for the dense phase. The obtained experimental data of pilot scale reactor was utilized for modeling validation. Investigation of fluidized bed operating conditions with the validated model was accomplished and the results indicated that higher reactor temperature, smaller zirconia size, and higher inlet gas velocity and concentration enhanced chlorination rate.

Keywords: Modeling, Zirconia, Fluidized bed reactor, Carbochlorination, Pilot scale

---

INTRODUCTION

The fluidized bed reactor has received considerable attention for producing zirconium tetrachloride, an intermediate in the production of zirconium metal, which is produced by carbochlorination of zirconia according to the following reaction:

$$ZrO_2+2Cl_2+2C \rightarrow ZrCl_4+2CO \quad (1)$$

The fluidized bed technique has many inherent advantages, including temperature uniformity, favorable heat transfer, ease of solid handling, low pressure drop, and operational flexibility.

Modeling of fluidized bed is necessary for design and scale up. Among many models employed, the hydrodynamic flow models are the most satisfactory for describing the performance of a bubbling fluidized bed[1]. This type of model describes and characterizes the parameters influencing the hydrodynamics of fluidized beds. Hydrodynamic models are divided into three categories, i.e., single, two- and three- phase model. A large number of these models are based on two phase concept of fluidization. In this category ofmodels, the fluidized bed is divided into two sections, bubble phase (rich in gas) and emulsion phase (rich in solids). Based on this model, Davidson-Harrison model [2], Partridge-Row model [3], the Kunii-Levenspiel model (Kunni and Levenspiel 1991)the Kato-Wen bubble assemblage model[4], the Chiba-Kobayashi bubble flow model [5], the shell model [6]have all been developed in accordance with different bubble dynamics.

There are some investigations that report on the chlorination of zirconia[7, 8, 9, 10, 11, 12, 13, 14]. Several mathematical models have been developed to simulate the fluid dynamics and reaction phenomena in the fluid bed. Jazini et al.[15] developed two two-phase hydrodynamic models for simulation of fluidized bed chlorination of zircon. They demonstrated that the plug-mixed model indicated a stronger correlation with experimental data. A mathematical description for the chlorination reaction of rutile was proposed [16]based on the gas-solid multi-phase reaction theory and a two-phase model for the fluidized bed. The results showed that the chlorination of natural rutile proceeded principally in the emulsion phase, and the reaction rate was mainly controlled by the surface reaction. Fuwa et al.[17]introduced the bubble assemblage model to interpret the selective chlorination of oxidized Ilmenite ore in the batch type fluidized bed. Rhee and Sohn[18]developed a more detailed model that incorporate the solid mixing. Youn and Park [19] developed a model to simulate the chlorination of rutile with coke in a fluidized bed.

The main objective of this work was to design and build a pilot-scale carbochlorination fluidized bed reactor with optimal operating conditions. The designed reactor consists of a novel middle layer structure which facilitates more uniform temperature in the reactor. Also an improved control system was provided for fine controlling of power input. Another objective of this work was to use a hydrodynamic two-phase model for simulation of the reactor. For authentication purposes, the experimental data were obtained from the pilot were used for modeling validation. Furthermore, the validated model was utilized to investigate and optimize the effects of initial zirconia particle size, inlet chlorine concentration, reactor temperature and superficial gas velocity time on reactor performance. Therefore, it is possible via the application of the obtained model to pinpoint the appropriate conditions for the reactor operation without any additional time consuming and expensive experiments.

EXPERIMENTAL SECTION

To obtain the necessary experimental data, a pilot scale carbochlorination reactor was designed and manufactured which is shown in Fig. 1. The reactor consists of two electrodes to introduce electric current into a fluidized bed of conductive particles. In the case of chlorination reactions, the bed of carbon particles provides both the necessary reductant and the heating means. The reactor system is made of a hard graphite chlorination reactor, a bed resistance heating unit, two condensing unit, and auxiliary equipment for supplying and measuring the gases, feed, and power to the system. The graphite chlorination reactor tapered from a 6.35-cm diameter at the bottom to 11.43 -cm in diameter at the top and was 123.19-cm high. A 1.27-cm hole in the bottom of reactor was used as a feed and fluidizing gas inlet. In order to achieve more uniform temperature throughout the reactor, a layer of fine graphite powder was built around the reactor. The second electrode for the heating system was at the center of the reactor. Openings at the top of the reactor also served as observation and exhaust ports. The reactor was mounted in a refractory-lined furnace shell with a 25-cm layer of fire brick insulation surrounding the reactor. The bed resistance heating system consisted of the electrode submerged in the bed material, the reactor wall which acts as the second electrode, a 800-AmperDC-power supply controlled by a variable transformer and auxiliary power measuring equipment. The volatilized chlorides were collected by two condensers.

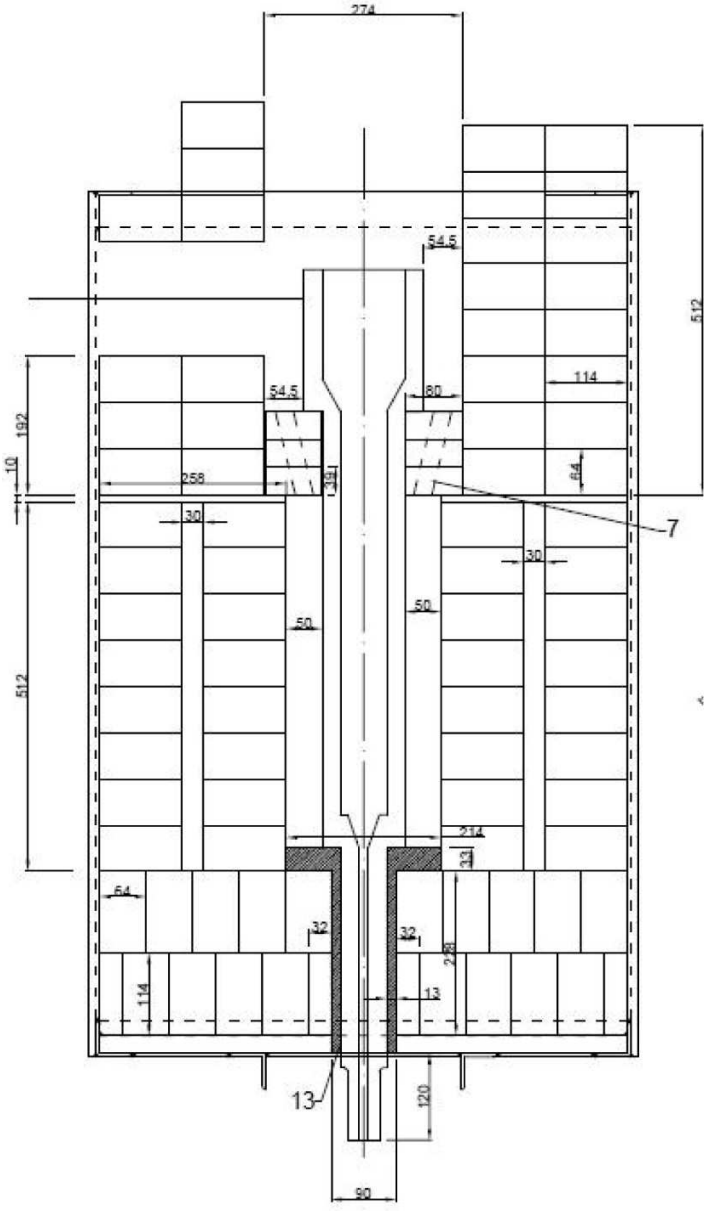

Figure 1- The structure of the pilot scale carbochlorination reactor with dimensions

The experiments were conducted in similar manners as follows: A 2000 g bed of well mixed petroleum coke and zirconia(20/80 W/W)was mixed with sucrose as a binder. Then the mixture was pressed and pelletized. Afterwards the pellets were dried and cooked. The cooked pelted were crushed and pulverized to the desired size. The obtained powder was put in to the chlorination reactor and fluidized with nitrogen. Power was supplied to the heating unit and the bed heated to operating temperature. When the desired temperature was reached in the chlorination reactor, the nitrogen flow was replaced with chlorine. The chlorine flow rate was 2 l/min, which provided superficial space velocities of 5 cm/s thorough the reactor. The chlorine flow and the power to the reactor then were shut off and the system was cooled in nitrogen. The flow diagram of the pilot is shown in Fig. 2.

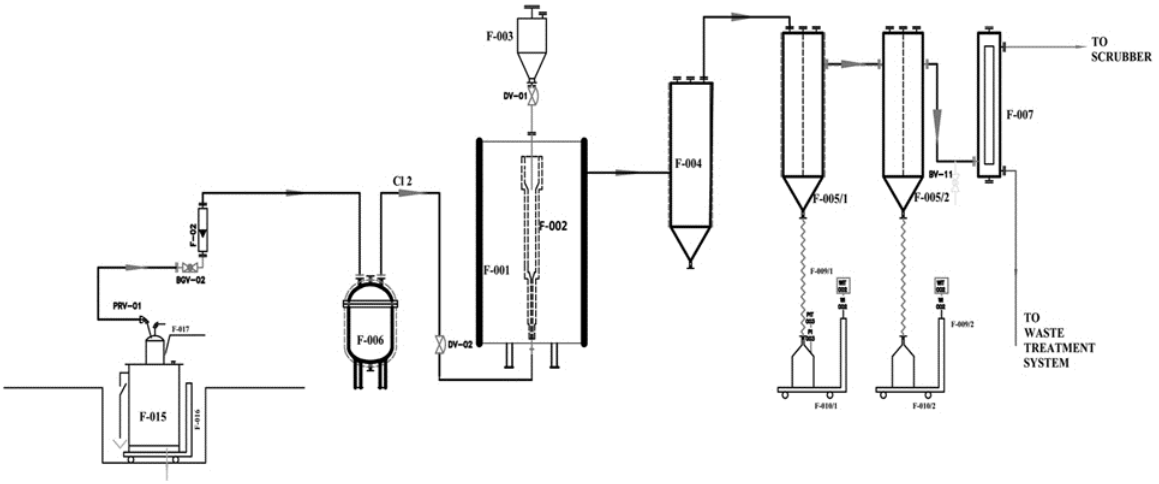

EQIPMENT NUMBER	F-001	F-002	F-003	F-004	F-005/1,2	F-006	F-007	F-009/1,2	F-010/1,2	F-017
EQUIPMENT NAME	FURNACE	ELECTROTERMAL FLUIDIZE BED	HOPPER	CYCLONE	CONDENSER	BUFFER	SCRUBBER	SCALE	SLAG TANK	CL2 CYLINDER
OPERATING TEMPERATURE(°C)	500~1200	500~1200	AMB	500	250	100	AMB	AMB	50	38
OPERATING PRESSURE(barg)	ATM	ATM	ATM	0.83	0.83	1	1	----	0.83	50
MATERIAL OF CONSTRUCTION	ASTM A283GR.C	HD-GRAPHITE	ASTM A283GR.C	SS 321	SS 321	s321/monel400	PVC	ST37/321	SS 321	ST37

Figure 2- Process flow diagram of the pilot scale carbochlorination reactor

The chlorination runs were evaluated on the basis of the relation of the weight and composition of the condensed volatile material to the quantities of the mixed oxide and carbon feed and chlorine used during the experiments.

1. Theory/Calculation

3.1 Model formulation

In developing the model, a fluidized bed with the following features and assumptions are considered:

1-The prepared feed powders are fed. They react with gases while being dragged up by the bubble and descending in the emulsion, and leave the bed by gas entrainment.

2-The bed consists of three regions: bubble, cloud and emulsion. The gases are exchanged among these regions. Considering uncertainties in estimation of gas-interchange parameter, the descriptions of fluidized bed was simplified by neglecting the mass transfer between the cloud and emulsion phase and considering the cloud as a part of emulsion phase. The exchange of gaseous species was accordingly simplified to be between the bubble and emulsion phase as had been carried out previously [20, 21, 22,23].

3-The gas compositions in the bubble and emulsion phases change with bed height, but the solids are uniformly mixed throughout the bed.

4-Horizontal variations of gas concentrations in each phase can be neglected.

5-The bed is operated under isothermal condition due to the rapid mixing in the bed.

6-Pressure drop along the bed height is neglected.

7-Volume exchange, in the gas phase according to the reaction stoichiometry is considered.

3.2 Mass balance on bubble and emulsion phase

The inlet gas is divided between the bubble and emulsion phase and gas is exchanged between them. Two models were formulated to describe the gas movement through the bed. In both of models, the flow pattern in bubble phase is considered as a plug flow, but for emulsion phase in P-P model, flow is plug and in P-M model flow is mixed. Fig. 3 visualizes the differential element in P-P & P-M model.

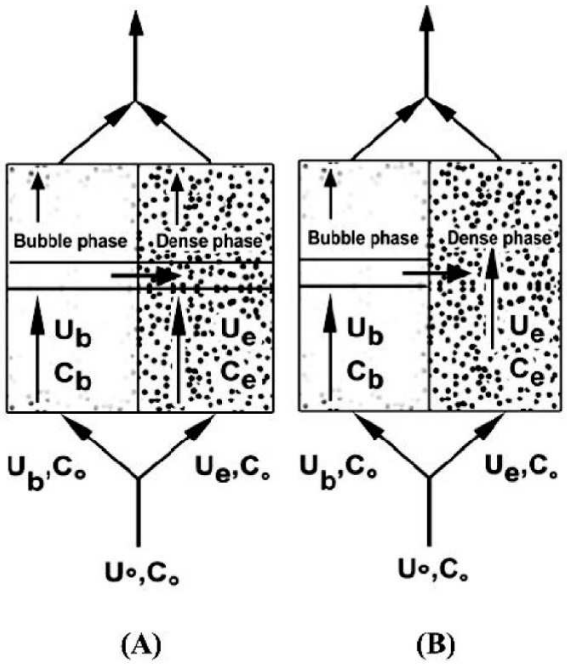

Figure 3- Differential element in bubble and emulsion phases. A) P-P model B) P-M model

The generalized steady-state mass balance equation for gas in either bubble or emulsion phase element is as follows:

$$(\text{Bulk flow in}) - (\text{Bulk flow out}) - (\text{Disappearance by reaction}) \pm (\text{Mass transfer}) = 0 \quad (2)$$

The reaction mechanism, kinetics, and rate equation developed via experimental correlation by Jena et al.[10]was used in the model. By applying Equation 2 to the system shown in Figure 1, for chlorine, in either bubble or emulsion phase element, the following equations will be derived for P-P model:

$$\frac{\partial X_b}{\partial z} = \frac{r_b}{u_{b0}C_{b0}} + \frac{K_{be}.\delta}{u_{b0}}\left(\frac{1-X_b}{1+\varepsilon_A X_b} - \frac{1-X_e}{1+\varepsilon_A X_e}\right) \quad (3)$$

$$\frac{\partial X_e}{\partial z} = \frac{r_e}{u_{e0}C_{e0}} - \frac{K_{be}.\delta}{u_{e0}}\left(\frac{1-X_b}{1+\varepsilon_A X_b} - \frac{1-X_e}{1+\varepsilon_A X_e}\right) \quad (4)$$

And for P-M model:

$$\frac{\partial X_b}{\partial z} = \frac{r_b}{u_{b0}C_{b0}} + \frac{K_{be}.\delta}{u_{b0}}\left(\frac{1-X_b}{1+\varepsilon_A X_b} - \frac{1-X_e}{1+\varepsilon_A X_e}\right) \quad (5)$$

$$F_{A0,e} - F_{A0,e}(1-X_e) - r_e.A.H_f + \int_0^{H_f} K_{be}.\delta\delta.A.\,{}_0\left(\frac{1-X_b}{1+\varepsilon_A X_b} - \frac{1-X_e}{1+\varepsilon_A X_e}\right)dz = 0 \quad (6)$$

3.3.Mass balance for solids:

A mass balance on zirconiaof size r_i gives (after discritization):

$$-K''(r_i)p_1(r_i) + w_z A\left[\frac{(p_1(r_i+1)R_t(C) - p_1(r_i)R_t(C)}{\Delta r_i}\right] = \frac{3w_z A p_1(r_i)R_t(C)}{r_i} \quad (7)$$

Solving for $p_1(r_i)$ leads to the following equation:

$$p_1(r_i) = \frac{\frac{w_z A p_1(r_i) R_t(C)}{\Delta r_i}}{K''(r_i) + w_z A R_t(C)\left[\frac{3}{r_i} + \frac{1}{\Delta r_i}\right]} \quad (8)$$

And $p_1(r_i)$ must satisfy the condition $\sum p_1(r_i)\Delta r_i = 1$, then:

$$\sum \left(\frac{w_z A p_1(r_i) R_t(C)}{K''(r_i) + w_z A R_t(C)\left[\frac{3}{r_i} + \frac{1}{\Delta r_i}\right]} \right) = 1 \quad (9)$$

The consumption rates of chlorine per unit volume of the fluidized bed in bubble and emulsion phase are:

$$r_b = \sum \frac{3 y_b w_z R_{b,b} p_1(r_i)}{r_i \rho_s \times 10^{-6}} \Delta r_i \quad (10)$$

$$r_e = \sum \frac{3 y_e w_z R_{b,e} p_1(r_i)}{r_i \rho_s \times 10^{-6}} \Delta r_i \quad (11)$$

Different formulations were obtained by Kunii and Levenspiel[24], Zhou and Sohn[25], and Overture and Reklaitis[26]with respect to the model developed in this work.

Entrainment rate of zirconiais calculated by the following relation:

$$F_{2z} = \sum K''(r_i) p_{1c}(r_i) \Delta r_i \quad (12)$$

Size distribution of zirconia in exit stream is evaluated by the following relation:

$$p_{2z}(r_i) = \frac{K''(r_i) p_{1z}(r_i)}{F_{2z}} \quad (13)$$

3.4. Energy balance:

The second law of thermodynamics for an adiabatic flow reactor is reduced to:

$$Q = \Delta H \quad (14)$$

Q is the amount of heat required for maintaining the reactor temperature at T. By using Fig.4, in mathematical symbol heat balance is as follow:

$$\Delta H = \sum_{i=1}^{n} n_{in} \int_{T_i}^{298} C_{pi} dT + \Delta H_{rxn} + \sum_{i=1}^{n} n_{out} \int_{298}^{To} C_{pi} dT \quad (15)$$

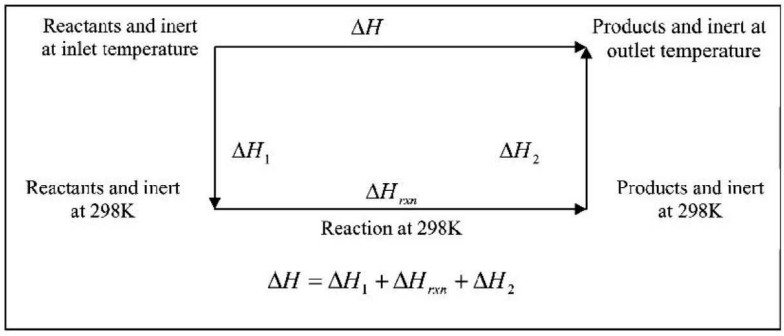

Figure 4- Thermodynamic path to calculate enthalpy change in bed

3.5 Method of numerical solution

The flow diagram for solving equations derived in previous section is shown in Fig. 5.Initial values of chlorine conversion and particle size distribution of zircon in bed are assumed, and then all coefficients and parameters in the model (some of them are shown in Table 1) and rate equation [17] were calculated based on the physical operating conditions.

Table 1- Methods used in calculation of parameters

Parameter	References
K_{be}	(Kunii and Levenspiel 1991)
H_f	(Kato and Wen 1969)
δ	(Cui et al. 2000)
Reaction rate	(Jena et al. 1999)
K''	(Wen and Chen 1982)

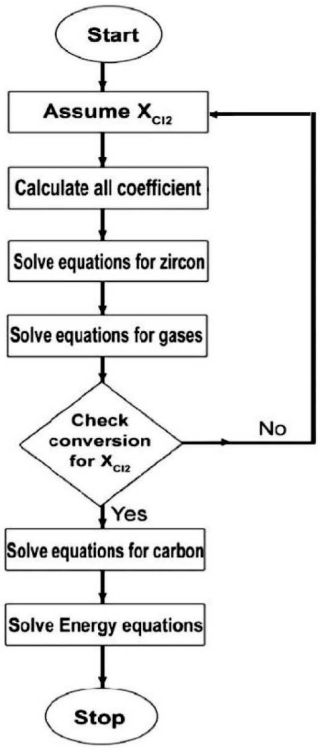

Figure 5- Flow diagram of the computer program

For a given carbon and zirconia mass in bed, the initial mass of zirconia (F_0), particle size distribution of powder in bed (p_1), entrainment rate of zirconia and carbon ($f_{2z,}$ f_{2c}), particle size distribution of zirconia in outlet gas stream (p_{2z}) are calculated from Equations 9, 8, 12 and 13, respectively. Using particle size distribution in bed, thus obtained, the consumption rate of reactant gas per unit volume of the bed in either the bubble or emulsion phase is calculated from Equations 10 and 11.Then Equations 3-4 (for P-P model) and 5-6 (for P-M model) are solved to obtain chlorine conversion along the bed height using the fourth-order Runge-Kutta method. Iterations are continued until the predetermined conversion criteria are met. The amount of heat needed for isothermal operation was calculated from Equation 15.

RESULTS AND DISCUSSION

4.1. Model validation

Table 2 shows comparisons between the experimental results and model predictions. This table shows that the results of the model have an excellent compatibility (5.2% relative errors) with experimental measurements. Therefore the validated model is used for further analysis of the reactor and to investigate the effects of initial particle size distribution of zirconia, reactor temperature, inlet gas velocity and concentration on the chlorine conversion and zirconia converted in bed.

Table2. Comparison of experimental values of pilot-scale chlorination reactor with model predictions

Exper. No.	Temperature (K)	Time (h)	Experimental Zirconia conversion (%)	predicted zirconia conversion (%)
RUN 1	1000	0.5	30	31.5
		1	65	68.4
		2	89	95.2
RUN 2	800	0.5	23	24.6
		1	48	51.1
		2	72	77
RUN 3	600	0.5	18	19.2
		1	35	36.5
		2	60	63.1

4.2. Modeling analysis of reactor effective variables

4.2.1. Effect of particle size on conversion

Fig.6 shows the effect of initial zirconia particle size on the chlorine conversion and converted zirconia by model prediction.

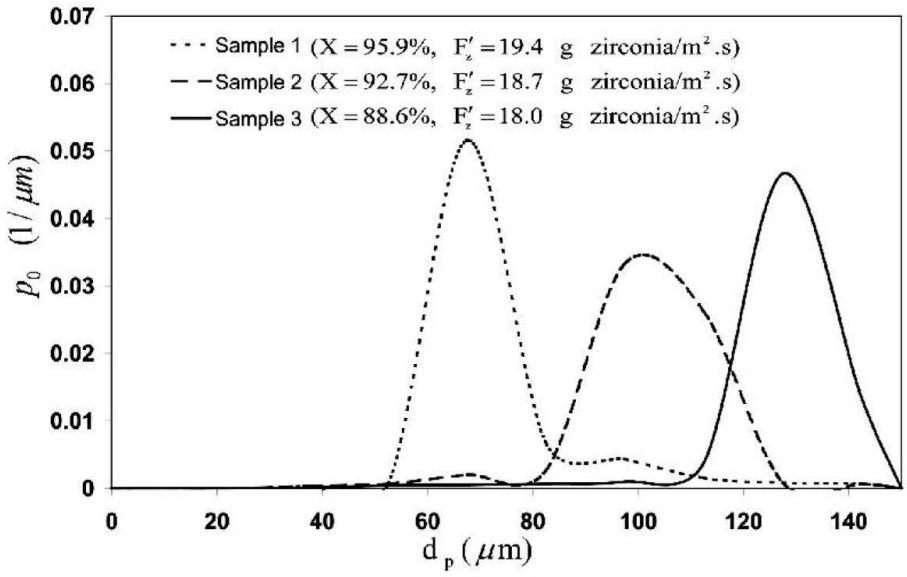

Figure 6- Effect of particle size (d_p) of inlet zirconia on chlorine conversion (X) and rate of converted zirconia ($F_z^{'}$: zirconia reacted per unit surface area of cross section of bed per unit time). P_0 = Size distribution function

The average diameters of the zirconia particles used in the model were chosen according to the physical conditions of the pilot plant reactor of this study and Spink et al. [27]. By using smaller zirconia nonporous particles such as 70 μm (average diameter distribution) with respect to 100 and 130 μm, the chlorine conversion and converted zirconia are increased and this is due to the availability of large surface for reaction in the case of smaller particles. For the case of 70 μm, the chlorine conversion of 95.9% and converted zirconia of 19.4 g zirconia/m^2.s were predicted by the model. Thus, smaller zirconia particle size is preferred according to the model predictions in order to obtain maximum chlorine conversion and flow rate of converted zirconia. But it is imperative to realize that there is a limit to what extent particle size can be reduced due to possible excessive entrainment of solid particles and also the lack of bubbling fluidization in the reactor and this must be optimized in conjunction with experimental observations.

4.2.2. Effect of inlet concentration and temperature on conversion

Fig.7 and 8 show the effect of concentration of inlet gas and reactor temperature on the chlorine conversion and converted zirconia by model prediction.

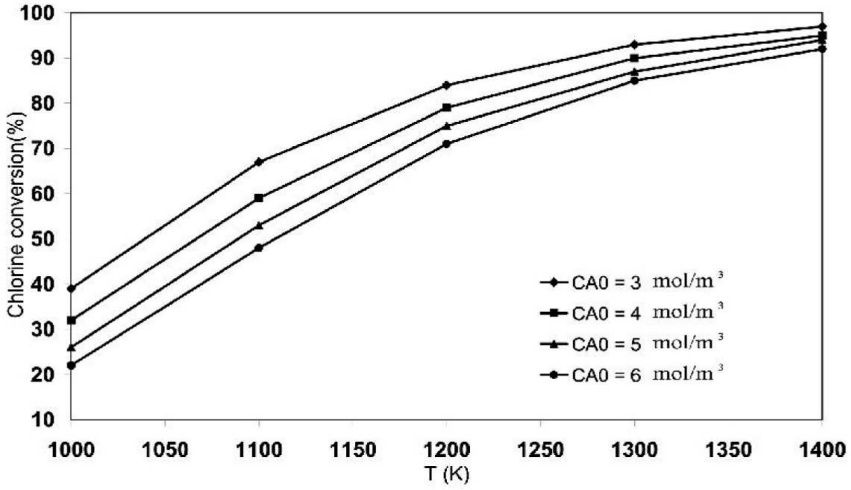

Figure 7- Effect of inlet chlorine concentration (C_{A0}) and reactor temperature (T) on the chlorine conversion

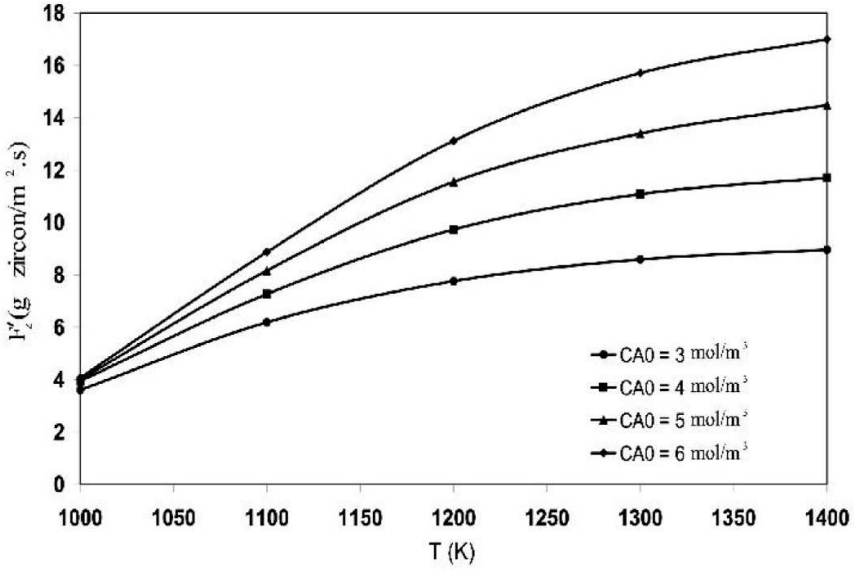

Figure 8- Effect of inlet chlorine concentration (C_{A0}) and reactor temperature (T) on the rate of zirconia converted in bed per unit cross section area of bed (F_z':)

Increasing temperature and inlet chlorine concentration cause higher reaction rate and consequently results in higher chlorine and zirconia consumption. For instance, for the inlet chlorine concentration of 3 mol/m^3 and the temperature range of 1000-1400 K, Fig.8 shows that the chlorine conversion is increased 55%. However, at a constant temperature, if inlet chlorine concentration is increased, higher zirconia consumption is obtained but at the same time chlorine conversion is decreased. This effect can be observed at 1200 K in which increasing chlorine concentration from 3 to 6mol/m^3 leads to 13%reduction in chlorine conversion and 38.4% enhancement in flow rate of converted zirconia consumption. This model prediction may be explained due to the low dependency of reaction rate with respect to chlorine concentration. The dependency of the reaction rate on the chlorine concentration is not significant at high concentrations because the reaction rate follows the Langmuir equation.

4.2.3. Effect of inlet gas velocity on conversion

Fig.9 shows the effect of inlet gas velocity on chlorine concentration in bubble phase along the bed predicted by the model. Higher gas velocity results in higher flow rate of converted zirconia consumption and moderate slope of chlorine concentration gradient in bubble phase. Enhancement of zirconia consumption flow rate (44.1%) is obtained by increasing gas velocity from 0.05 to 0.1 m/s. When gas velocity is increased, bubble size is increased and reduction of gas transfer rate between bubble and emulsion is observed, therefore the behavior of the bed is alike a plug flow reactor and this results in higher concentration along the bed and consequently higher reaction rate. Overall, this leads to appropriate mass transfer and hydrodynamic conditions in terms of obtainable conversion.

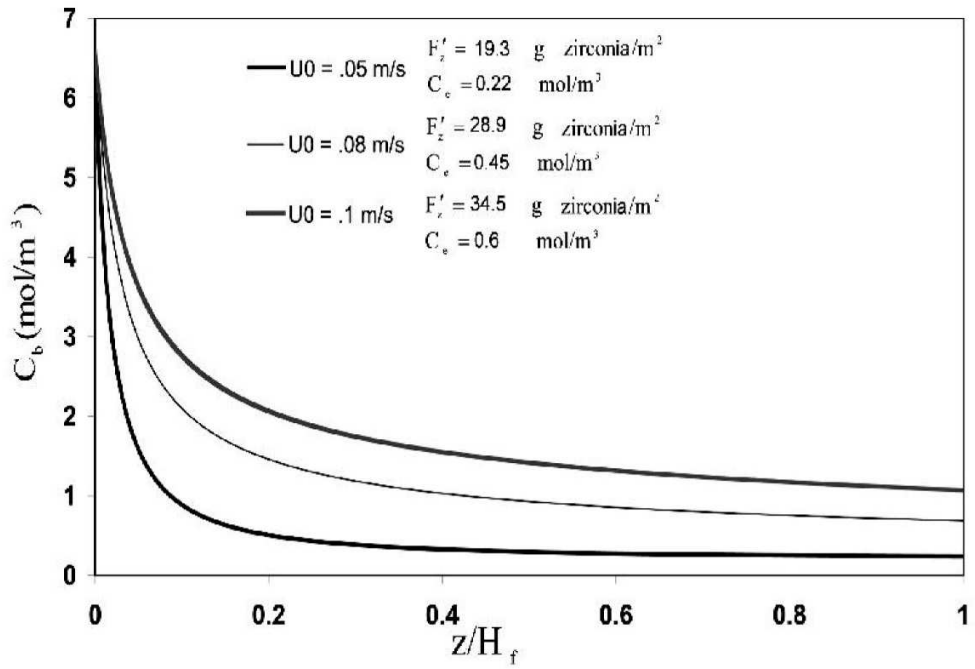

Figure 9- Effect of inlet gas velocity (U_0) on chlorine concentration gradient (C_b) and converted zirconia along the bed in bed per unit cross section area of bed ($\acute{F}_z$). z: bed height. H_f: total bed height.

4.2.4. Effect of inlet gas velocity on final zirconia size distribution

Fig.10 shows the effect of inlet gas velocity on final zirconia size distribution in bed via model prediction. The gas velocity operating range (0.05-0.1 m/s) was chosen such that bubbling fluidization can be sustained throughout the process. The results ofFig.10 demonstrate that there is no dependency of final particle size distribution on gas velocity in which the average particle size distribution of 70 μm was obtained for the three different gas velocity. This indicates that solid dynamics is much slower than gas phase dynamics because, as mentioned in Fig.9, inlet gas velocity has a significant effect on chlorine concentration gradient. At the conditions ofFig.10, the particle size distribution of elutriated zirconia is the same as bed because gas velocity is higher than terminal velocity of all particles and thus all of them could be entrained by gas and it can be concluded that the elutriated particles is a sample of particles in the bed. Knowing the zirconia particle size distribution in the bed, which is a true representative of elutriated particles, is vital to design the separation apparatus beyond the reactor.

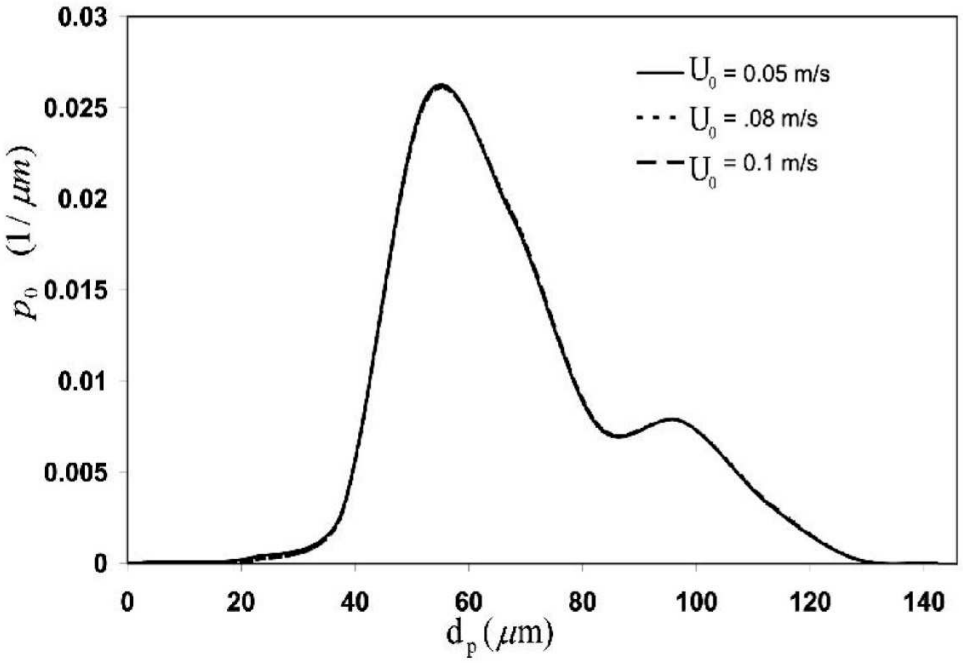

Figure 10- Effect of inlet gas velocity (U0) on zirconia particle size distribution in bed. P_0: Size distribution function

CONCLUSION

A pilot scale carbochlorination reactor was designed, manufactured and modeled. The experimental data were obtained from the pilot were utilized for the validation of the developed model. The model resulted in numerical predictions which show a close compatibility with the experimental data. Furthermore, the validated model was used for optimization of the operating variables. Using the authenticated model, the effects of different operating conditions were investigated and the results demonstrated that small zirconia size of 70 μm, high inlet gas velocity of 0.1 m/s, inlet chlorine concentration of 6 mol/m^{3}and reactor temperature of 1400 K enhanced the chlorination rate.

Acknowledgments
The financial support provided for this project by Isfahan University of Technology (IUT) is gratefully acknowledged.

REFERENCES

[1] O Levenspiel. Chemical reaction engineering. Wiley, **1972**.
[2] **JF Davidson:** Fluidized Particles, pp. 173-196, in: Guazzelli, E. and Oger, L. (Ed.), Mobile Particulate Systems, vol.287. Springer Netherlands (1995).
[3] PN Rowe BA Partridge. *Chem. Eng. Res. Des.*, **1997**, 75, Supplement, S116-S134.
[4] K Kato CY Wen. *Chem. Eng. Sci.*, **1969**, 24, 1351-1369.
[5] H Farag; M Ossman; M Mansour Y Farid. *Int. J. Ind. Chem.*, **2013**, 4, 1-10.
[6] SK Kanholy; J Chodak; BY Lattimer F Battaglia. *J. Fluids Eng.*, **2012**, 134, 111303-111303.
[7] O Biceroglu WH Gauvin. *AIChE J.*, **1980**, 26, 734-743.
[8] O Bicerolu WH Gauvin. *Can. J. Chem. Eng.*, **1980**, 58, 357-366.
[9] E Bohe A M Pasquevich D. *Ber. Bunsen-Ges.*, **1995**, 99, 1553-1558.
[10] PK Jena; EA Brocchi MLD Reis. *Metall. Mater. Trans. B*, **1999**, 30, 375-381.
[11] AJ O'Reilly; ID Doig JS Ratcliffe. *J. Inorg. Nucl. Chem.*, **1972**, 34, 2487-2495.
[12] DM Pasquevich VT Amorebieta. *Ber. Ges. Phys. Chem*, **1992**, 96, 530-533.
[13] DM Pasquevich A Caneiro. *Thermochim. Acta*, **1989**, 156, 275-283.
[14] DM Pasquevich; JA Gamboa A Caneiro. *Thermochim. Acta*, **1992**, 209, 209-222.
[15] MH Jazini; SM Ghoreishi AA Dadkhah. *Metall. Mater. Trans. B*, **2010**, 41, 248-254.

[16] L-p Niu; T-a Zhang; P-y Ni; G-z LÜ K Ouyang. *Trans. of Nonferrous Met. Soc.* . .**2013**, 23, 3448-3455.
[17] A Fuwa; E Kimura S Fukushima. *Metall. Mater. Trans. B*, **1978**, 9, 643-652.
[18] KI Rhee HY Sohn. *Metall. Mater. Trans. B*, **1990**, 21, 341-347.
[19] I-J Youn K Park. *Metall. Mater. Trans. B*, **1989**, 20, 959-966.
[20] P Ammendola; R Chirone; G Ruoppolo; G Russo R Solimene. *Int. J. Hyd. En.*, **2008**, 33, 2679-2694.
[21] JP Constantineau; JR Grace; CJ Lim GG Richards. *Chem. Eng. Sci.*, **2007**, 62, 70-81.
[22] A Kiashemshaki; N Mostoufi R Sotudeh-Gharebagh. *Chem. Eng. Sci*., **2006**, 61, 3997-4006.
[23] DA Nemtsov A Zabaniotou. *Chem. Eng. J.*, **2008**, 143, 10-31.
[24] D Kunii O Levenspiel. Fluidization Engineering. Butterworth-Heinemann, **1991**.
[25] L Zhou HY Sohn. *AIChE J.*, **1996**, 42, 3102-3112.
[26] BW Overturf GV Reklaitis. *AIChE J.*, **1983**, 29, 813-820.
[27] DR Spink; JW Cookston JE Hanway, Jr. Fludized bed chlorination of zirconium-bearing materials, **1968**.